"The Dark Arts are many, varied, ever-changing, and eternal. Fighting them is like fighting a many-headed monster, which, each time a neck is severed, sprouts a head even fiercer and cleverer than before. You are fighting that which is unfixed, mutating,indestructible."

Severus Snape in "Harry Potter and the Half-Blood Prince"

2

Neutrino phenomenology and scalar dark matter with inverse and type II seesaw

---

In the second chapter we present a TeV scale seesaw mechanism for exploring the dark matter and neutrino phenomenology in the light of recent neutrino and cosmology data. A unique realization of the Inverse seesaw (ISS) mechanism with A_4 flavor symmetry is being implemented as a leading contribution to the light neutrino mass matrix which usually yields vanishing reactor angle θ_{13}. Making use of a non-diagonal structure of Dirac neutrino mass matrix and 3σ values of mass square differences the neutrino mass matrix is parameterized in terms of Dirac Yukawa coupling "y". We then use type II seesaw mechanism as a correction which turns out to be active to have a non-vanishing reactor mixing angle without much disturbing the other neutrino oscillation parameters. Then we constrain a common parameter space satisfying the non-zero θ_{13}, Yukawa coupling and the relic abundance of dark matter. Contributions of neutrinoless double beta decay are also included for standard light neutrino interaction. This study may have relevance in future neutrino and Dark Matter experiments.

2.1 Introduction

The link between neutrino oscillation and modern cosmology needs an elucidation since both of them infer physics beyond Standard Model (BSM). Several theories have been deciphered to bridge between these two separate sectors of particle physics and cosmology [1]. There is now a plethora of evidences in support of the existence of dark matter (DM) which constructs approximately one-fourth of the energy density of the universe [2–5]. Despite a number of recent studies of simplified DM models their nature remains rather elusive. Even the most successful Standard Model (SM) also does not furnish any signature of dark matter candidates and their properties. This is one of the pressing problems in both high energy physics and cosmology. Therefore, searching for a concrete realization to provide a hint towards physics BSM will be of utmost interest. It will be more fascinating if the discovery of neutrino oscillation and the existence of DM can be framed within a single particle physics model.

Even though astrophysical and cosmological observations, strongly suggest about the Presence of DM in the universe, the exact particle nature of DM is still unidentified. Planck 2013 data [5] says that, DM composes 26.8% of the energy density of the present universe, which predicts the present abundance (familiar as relic abundance) of DM as

$$\Omega_{DM}h^2 = 0.1187 \pm 0.0017, \tag{2.1.1}$$

where Ω implies the density parameter, Hubble parameter/100= is denoted as $h =$ [6]. Authors in [7] proposed a ten-point test that new particle has to satisfy so that it can be regarded as a potential DM candidates. The existence of dark matter is universally accepted, its nature remains elusive. It is usually assumed to be a single particle, but it may also be more than one. In specific models, it is often considered to be a fermion, scalar or vector [8]. Among the requirements the potential DM candidate must meet, the stability is protected by invoking some parity symmetry like Z_2 which is supposed to appear as a residual of a discrete flavor symmetry. There have been extensive studies in this field adopting various flavor symmetry groups [9–11]. We have plenty of examples where different kinds

of DM were extensively studied with their stability in several ways. Recently connection between neutrino and the DM, using various flavor symmetries is drawing more attention in particle physics and cosmology. Here also we present a picture to construct a bridge between these two different sectors of particle physics adopting the A_4 based ISS realization. The most peculiar signatures of the ISS scenario are the additional decay channels of the Higgs boson into a heavy and ordinary neutrino, which confirms the SM particles to be a gateway to the scalar DM. In order for the SM particles being a portal to the dark sector, there must be at least two particles, one fermion and one boson in the dark sector. Here in our model Higgs boson, is considered as a DM candidate, couples with SM neutrino through a right handed neutrino. Two neutral components of this Higgs which is a triplet under A_4 is responsible in making correlation with neutrino mass and dark matter. A remnant Z_2 symmetry can explain the stability issue of the potential dark matter. This Z_2 symmetry also prevents the interaction of other particle contents of the model with the DM. Apart from the stability issue one more important test it must pass is to satisfy the observed relic density given by Eq. (2.1.1). For getting the correct relic abundance we require to take the DM mass from 50 GeV onwards. The Yukawa, which is responsible in making correlation between neutrino mass and DM coupling also needs to be fixed in such a way that the potential DM candidate gives rise to correct relic abundance.

Several seesaw mechanisms have shown a promising role in explaining neutrino mass and mixing. The inverse Seesaw (ISS) has been found to be an entirely different realization, which delicately attempts for the generation of a tiny neutrino mass at the cost of proposing the RH neutrino masses at the TeV scale which may have a better collider accessibility in near future. The essence of the ISS lies in the fact that, the double appearance of the mass scale associated with M in the denominator of the inverse seesaw formula allows it (M) to take a mass scale, which is much lighter than the one associated with the type I seesaw mechanism. Which in turn renders us with sub-eV scale SM neutrinos, at the cost of electroweak scale m_D, TeV scale M and keV scale μ, as explained in [12]. This

RH neutrino mass at TeV scale helps us to get the required mediator mass in order to obtain the appropriate relic abundance of relics. In addition to the ISS we are working with the Type II seesaw mechanism which turns out to be instrumental to have the non-vanishing reactor mixing angle. Both the inverse and type II seesaw are realized adopting the A_4 flavor symmetry. Then we have also studied the effective mass prediction to neutrinoless double beta decay (NDBD) for standard contribution.

We organize this chapter as follows. In section. 2.2 we present our model. Section 2.3 provides the stability issue of DM. Non-zero reactor angle is explained in the section 2.4. Section 2.5 has been presented with the analysis on Neutrinoless double beta decay. Section 2.6 offers the observation of the Relic abundance of DM in the background of the presented model. We have kept the numerical analysis in section 2.7. Finally, in section 2.8 we end up with our conclusion.

2.2 Neutrino mass model with various seesaw scenarios

2.2.1 Inverse seesaw mechanism

In our work we focus on the simplest ISS mechanism which is able to open up a new window to look for a comparatively lower right handed neutrino mass scale than the one present in type I seesaw [12–19]. The fulfillment of the ISS scheme requires the SM fermion sector to be extended by the inclusion of three RH neutrinos N and three additional neutral fermion singlets S_{iL}, where $i = 1, 2, 3$. It is worth stating that, the implementation of the ISS allows us to make use of extra symmetries in order to provide the neutrinos the following bilinear terms,

$$\mathcal{L} = -\bar{\nu}_L m_D N - \bar{S}_L M N - \frac{1}{2}\bar{S}_L \mu S_L^C + H.C., \tag{2.2.1}$$

The above Lagrangian implies a 9×9 leptonic mass matrix,

$$M_\nu = \begin{pmatrix} 0 & m_D & 0 \\ m_D^T & 0 & M \\ 0 & M^T & \mu \end{pmatrix}. \tag{2.2.2}$$

In spite of its many phenomenological successes the ISS has a drawback that the RH mass term in the $M_{\nu_{22}}$ entry of M_ν is allowed by symmetries. This is a typical problem of inverse seesaw models. But it is prevented here by using Z_3 symmetry. After block diagonalization of the Eq. (2.2.2) we get the lightest neutrino mass eigenvalue as ,

$$m_\nu^I = m_D(M^T)^{-1}\mu M^{-1}m_D^T, \tag{2.2.3}$$

which is considered as the leading contribution to the light neutrino mass. Unlike the GUT scale seesaw mechanism, the ISS still needs an appropriate ground where the six new neutrinos could find their places in the elemental particle content and normally can get a mass term.

Non Abelian discrete flavor symmetries have played an important role in particle physics since long. In particular the symmetry group A_4 have been immensely found of utmost operation [20–24]. In this work we have analyzed the model presented by the authors in [9], extended with additional flavons with inverse and type II seesaw. We summarize the A_4 based ISS model by assigning the matter fields as shown in Table 2.1. We introduce four RH neutrinos, three of which $N = (N_1, N_2, N_3)$ are supposed to be a triplet of A_4 and the rest as a singlet N_4. We assign the SM type Higgs η to the A_4 triplet, which is considered as a DM candidate in the present analysis. We have four additional SM fermion singlets among which 'S' is transforming as A_4 triplet and S_4 as A_4 singlet. To get a desired neutrino mass matrix structure we are extending the Higgs sector by introducing six more Higgs fields, boosted by two additional symmetries Z_2 and Z_3 whose quantum numbers are given in Table 2.1. We construct the ISS mass matrices using the multiplication rules of A_4 as given in Section 1.8 of Chapter 1.

2.2.2 Type II seesaw with triplet Higgs

To implement the type II seesaw mechanism, the SM is extended by the addition of a new $SU(2)_L$ triplet scalar field Δ whose 2×2 matrix representation is given

as

$$\Delta = \begin{pmatrix} \Delta^+/\sqrt{2} & \Delta^{++} \\ \Delta^0 & \Delta^+/\sqrt{2} \end{pmatrix}, \tag{2.2.4}$$

The VEV of the SM Higgs $< \phi_0 >= v/\sqrt{2}$, the trilinear mass term $\mu_{\phi\Delta}$ generate an induced VEV for the Higgs triplet as $\Delta^0 = v_\Delta\sqrt{2}$ where, $v_\Delta \simeq \mu_{\phi\Delta}v^2/\sqrt{2}M_\Delta^2$ [25]. The light neutrino mass is contributed by the type II seesaw mechanism in the following manner

$$m_{LL}^{II} = f_\nu v_\Delta, \tag{2.2.5}$$

where the analytic formula for induced VEV for the neutral component of the Higgs scalar triplet, derived by minimizing the scalar potential [25], is

$$v_\Delta \equiv \langle \Delta^0 \rangle = \frac{\mu_{\phi\Delta}v^2}{\sqrt{2}M_\Delta^2} \tag{2.2.6}$$

In the low scale type II seesaw which is dynamic at the TeV scale, we can consider a very small value of the trilinear mass parameter to be

$$\mu_{\phi\Delta} \simeq 10^{-8}GeV.$$

The sub-eV scale neutrino mass coming from type II seesaw mechanism constrains the corresponding Majorana Yukawa coupling as

$$f_\nu^2 < 1.4 \times 10^{-5}(\frac{M_\Delta}{1TeV})$$

Within the reasonable value of $f_\nu \simeq 10^{-2}$, the triplet Higgs scalar VEV is $v_\Delta \simeq 10^{-7}GeV$ which is in agreement with oscillation data. It is worth to note here that the tiny trilinear mass parameter $\mu_{\phi\Delta}$ controls the neutrino overall mass scale, but does not play any role in the couplings with the fermions. The structure of the matrix m_{LL}^{II}, with $w = f_\nu v_\Delta$ is explained in Section. 2.4.

2.3 Stabilizing the dark matter

An elegant way to establish the DM stability is by invoking a parity symmetry like Z_2. Here is an attempt to search for a theory which is responsible for explaining neutrino phenomenology and dark matter stability as well. The $A_4 \times Z_2 \times Z_3$

symmetry here only allows the coupling of the η with the singlet RH neutrinos rather than with charged fermions or quarks. It is worth noting that the alignment $\langle\eta\rangle \sim (1,0,0)$ breaks $A_4 \times Z_2 \times Z_3$ to Z_2 since $(1,0,0)$ remains manifestly invariant under one of the generators of the group A_4. In this manner spontaneously breaking of the symmetry, obeyed by the bigger group $A_4 \times Z_2 \times Z_3$ to Z_2 confirms the DM stability. The stability of the DM candidate is guaranteed by this remnant symmetry. The Z_2 residual symmetry is defined by

$$N_2 \to -N_2, S_2 \to -S_2, \eta_2 \to -\eta_2$$
$$N_3 \to -N_3, S_3 \to -S_3, \eta_3 \to -\eta_3$$

The leading order Yukawa Lagrangian for the neutrino part is given by the following equation.

$$\begin{aligned}\mathcal{L}_\nu^I = y_1^\nu L_e(N\eta)_1 + y_2^\nu L_\mu(N\eta)_{1''} + y_3^\nu L_\tau(N\eta)_{1'} + y_4^\nu L_e N_4 h \\ + y_s(SS)\phi_s + y_s' S_4 S_4 \phi_s + y_R(NS)\phi_R + y_R' N_4 S_4 \phi_R.\end{aligned} \tag{2.3.1}$$

	L_e	L_μ	L_τ	l_e^c	l_μ^c	l_τ^c	N	N_4	h	η	S_4	S	ϕ_R	ϕ_s	ζ	ξ	Δ
$SU(2)_L$	2	2	2	1	1	1	1	1	2	2	1	1	1	1	1	1	3
A_4	1	$1'$	$1''$	1	$1''$	$1'$	3	1	1	3	1	3	1	1	$1'$	$1''$	1
Z_2	1	1	1	1	1	1	1	1	1	1	-1	-1	-1	1	1	1	1
Z_3	ω	ω	ω	ω^2	ω^2	ω^2	ω^2	ω^2	1	1	ω	ω	1	ω	1	1	ω

Table 2.1: Particles and their quantum numbers under $SU(2)_L$ symmetry, and A_4, Z_2, Z_3 flavour symmetry groups

The following flavon alignments help us to get a desired neutrino mass matrix.

$$\langle\Phi_R\rangle = v_R, \langle\Phi_s\rangle = v_s, \langle h\rangle = v_h, \langle\eta\rangle = v_\eta(1,0,0).$$

It is clear from the Eq. (2.3.2) and Eq. (2.3.3) that, m_D is related to v_η and v_h, M is determined by the VEV v_R. From this, the order of magnitude involved in the Eq. (2.2.3) is so, that $m_\nu \propto \frac{(v_\eta+v_h)^2}{v_R^2}\mu$. Here v_η and v_h are of the order

of electroweak breaking, v_R is of the order of TeV scale. Therefore, to get m_ν in sub-eV, μ which is coming from the VEV of Φ_S should be of the order of keV. The two components of η are not generating the VEV [9], considered potential DM candidate. Decomposition of the following terms present in the Eq. (2.3.1) has been shown as follows

$$y_s(SS)\phi_s = y_s(S_1S_1 + S_2S_2 + S_3S_3)\phi_s,$$
$$y_R(NS)\phi_R = y_R(N_1S_1 + N_2S_2 + N_3S_3)\phi_R.$$

The chosen flavon alignments and the A_4 product rules allow us to have the Yukawa coupling matrices as follows

$$m_D = \begin{pmatrix} y_1^\nu\langle\eta\rangle & 0 & 0 & y_4^\nu\langle h\rangle \\ y_2^\nu\langle\eta\rangle & 0 & 0 & 0 \\ y_3^\nu\langle\eta\rangle & 0 & 0 & 0 \end{pmatrix} = \begin{pmatrix} x_1a & 0 & 0 & y_1b \\ x_2a & 0 & 0 & 0 \\ x_3a & 0 & 0 & 0 \end{pmatrix}, \tag{2.3.2}$$

$$M = \begin{pmatrix} y_R\langle\phi_R\rangle & 0 & 0 & 0 \\ 0 & y_R\langle\phi_R\rangle & 0 & 0 \\ 0 & 0 & y_R\langle\phi_R\rangle & 0 \\ 0 & 0 & 0 & y_R'\langle\phi_R\rangle \end{pmatrix} = \begin{pmatrix} M_1 & 0 & 0 & 0 \\ 0 & M_1 & 0 & 0 \\ 0 & 0 & M_1 & 0 \\ 0 & 0 & 0 & M_2 \end{pmatrix}, \tag{2.3.3}$$

$$\mu_s = \begin{pmatrix} y_s\langle\phi_s\rangle & 0 & 0 & 0 \\ 0 & y_s\langle\phi_s\rangle & 0 & 0 \\ 0 & 0 & y_s\langle\phi_s\rangle & 0 \\ 0 & 0 & 0 & y_s'\langle\phi_s\rangle \end{pmatrix} = \begin{pmatrix} \mu_1 & 0 & 0 & 0 \\ 0 & \mu_1 & 0 & 0 \\ 0 & 0 & \mu_1 & 0 \\ 0 & 0 & 0 & \mu_2 \end{pmatrix}, \tag{2.3.4}$$

The light neutrino mass matrix as produced by the above three matrices under the ISS framework is given by

$$m_\nu = \begin{pmatrix} \frac{y_1^2b^2\mu_2}{M_2^2} + \frac{a^2x_1^2\mu_1}{M_1^2} & \frac{a^2x_1x_2\mu_1}{M_1^2} & \frac{a^2x_1x_3\mu_1}{M_1^2} \\ \frac{a^2x_1x_2\mu_1}{M_1^2} & \frac{a^2x_2^2\mu_1}{M_1^2} & \frac{a^2x_2x_3\mu_1}{M_1^2} \\ \frac{a^2x_1x_3\mu_1}{M_1^2} & \frac{a^2x_2x_3\mu_1}{M_1^2} & \frac{a^2x_3^2\mu_1}{M_1^2} \end{pmatrix}. \tag{2.3.5}$$

The assigned A_4 charge of this Higgs triplet η restricts the interaction of η with the charged leptons. In this model the charged leptons gain mass from the

Lagrangian give by

$$\mathcal{L}_l^I = y_e L_e l_e^c h + y_\mu L_\mu l_\mu^c h + y_\tau L_\tau l_\tau^c h \tag{2.3.6}$$

Following is the mass matrix for charged leptons.

$$m_l = \begin{pmatrix} y_e\langle h\rangle & 0 & 0 \\ 0 & y_\mu\langle h\rangle & 0 \\ 0 & 0 & y_\tau\langle h\rangle \end{pmatrix} \tag{2.3.7}$$

2.4 The reactor mixing angle

It is needless to say that there is a menagerie of theories, put forward in establishing the θ_{13} as having a nonzero value. Here also we are trying to present such a picture by including a perturbation called type II perturbation to the Lagrangian given by Eq. (2.3.1) which is realized within the type II seesaw mechanism [25–30]. The type II seesaw Lagrangian is followed by this term

$$\mathcal{L}^{II} = f_\nu(L_e L_\tau + L_\mu L_\mu + L_\tau L_e)\zeta\frac{\Delta}{\Lambda} + f_\nu(L_e L_\mu + L_\mu L_e + L_\tau L_\tau)\xi\frac{\Delta}{\Lambda} \tag{2.4.1}$$

Where, Λ represents the cutoff scale. With the type II perturbation the Lagrangian takes the following form,

$$\begin{aligned}\mathcal{L} = {} & y_e L_e l_e^c h + y_\mu L_\mu l_\mu^c h + y_\tau L_\tau l_\tau^c h + y_1^\nu L_e(N\eta)_1 + y_2^\nu L_\mu(N\eta)_{1''} + y_3^\nu L_\tau(N\eta)_{1'} \\ & + y_4^\nu L_e N_4 h + y_s(SS)\phi_s + y_s' S_4 S_4 \phi_s + y_R(NS)\phi_R + y_R' N_4 S_4 \phi_R \\ \mathcal{L}^{II} = {} & f_\nu(L_e L_\tau + L_\mu L_\mu + L_\tau L_e)\zeta\frac{\Delta}{\Lambda} + f_\nu(L_e L_\mu + L_\mu L_e + L_\tau L_\tau)\xi\frac{\Delta}{\Lambda}.\end{aligned} \tag{2.4.2}$$

The last two terms represent the perturbation to the leading order terms in the above Lagrangian giving rise to non-zero θ_{13}. Here we have implemented the A_4 group to explain the structure of the type II seesaw neutrino mass matrix given by Eq. (2.4.3). The triplet Higgs field Δ_L is supposed to be an A_4 singlet. Two more flavon fields ζ and ξ have been introduced which are assumed to transform as A_4 singlets as summarized in the Table. 2.1. The flavon alignments which help in constructing the m_{LL}^{II} matrix are as follows

$$\langle\Delta\rangle \sim v_\Delta, \quad \langle\zeta\rangle \sim v_\zeta, \quad \langle\xi\rangle \sim v_\xi$$

. ζ and ξ are assumed to take the VEV in the same scale $v_\zeta = v_\xi = \Lambda$. With these flavon alignments the structure of mass matrix m_{LL}^{II} will take the form

$$m_{LL}^{II} = \begin{pmatrix} 0 & -w & w \\ -w & w & 0 \\ w & 0 & -w \end{pmatrix}. \tag{2.4.3}$$

2.5 Neutrinoless double beta decay

The time period for neutrinoless double beta ($0\nu\beta\beta$) decay rate is exactly proportional to the effective neutrino mass square $|m_\nu^{ee}|^2$ (for a detail please see [31–33]). Which implies that in determining the time period for NDBD, the effective mass plays a non-trivial role in the scenario of three generations of neutrinos. The effective neutrino mass can be given by

$$|m_\nu^{ee}| = |U_{ei}^2 m_i|, \tag{2.5.1}$$

In addition to this, following non-standard contributions become transparent in

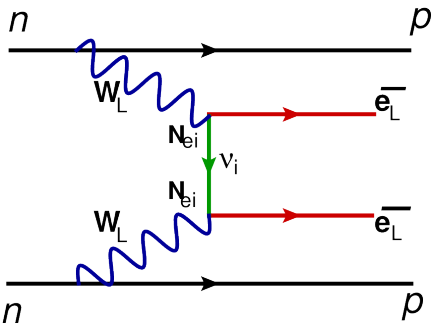

Figure 2.1: Feynman diagram representing $0\nu\beta\beta$ Decay because of light neutrino exchanges.

the present model.

- Two separate contributions due to light and heavy neutrino exchanges to $0\nu\beta\beta$ come into play. And this event is established by writing the flavor eigenstates as a linear combination of light and heavy mass eigenstates. The only contribution that becomes effective in the ISS regime comes from the contribution due to light neutrino exchanges.

$$\nu_\alpha = N_{\alpha i}\nu_i + U_{\alpha j}\xi_j, \tag{2.5.2}$$

where, $N_{\alpha i}$ and $U_{\alpha j}$ are the mixing matrices for light and heavy neutrino respectively. $|m_\nu^{ee}|$ takes distinct values depending on the framework (quasi degenerate or normal/inverted hierarchies), the neutrino mass states are in. Now considering the light neutrino contribution (the only contribution for ISS in this model), the key formula which determines the effective neutrino mass is

$$m_{\nu,LL}^{ee} \simeq U_{e1}^2 m_1 + U_{e2}^2 e^{2i\alpha} m_2 + U_{e3}^2 e^{2i\beta} m_3. \tag{2.5.3}$$

- The triplet Higgs contribution from the type II seesaw is of the order of $10^{-13} m_i$ which is much smaller as compared to the leading contributions.

Of special importance is the fact that, the chosen value of Yukawa coupling giving rise to the observed relic abundance of our DM candidate, constrains the lightest neutrino mass significantly in the presented forum. The fine tuned Yukawa couplings $(0.994 - 1)$ is noticed to play a vital role in achieving the lightest neutrino mass and in turn to get the effective neutrino mass prediction within the GERDA bound $(0.5eV)$. The type II perturbation strength is found to play some role in giving $m_{lightest}$ within the PLANK bound (0.065 eV for IH). The introduced model also evinces the role of $U_{\rm PMNS}$ matrix elements and the lightest neutrino mass as $|m_\nu^{ee}|$ is dependent upon them.

2.6 Relic density of dark matter

The relic abundance of a DM particle χ is given by the Boltzmann equation [34–37]

$$\frac{dn_\chi}{dt} + 3Hn_\chi = - < \sigma v > (n_\chi^2 - (n_\chi^{eqb})^2), \tag{2.6.1}$$

where n_χ is the dark matter (χ) number density with n_χ^{eqb} as the equilibrium number density of χ, in thermal equilibrium. The Hubble rate is denoted as H and $< \sigma v >$ is the thermally averaged annihilation cross-section of the DM χ. Numerical solution of the Boltzmann equation is given by [35]

$$\Omega_\chi h^2 \approx \frac{1.04 \times 10^9 x_F}{M_{pl}\sqrt{g_*}(a + 3b/x_F)}, \tag{2.6.2}$$

where $x_F = \frac{m_\chi}{T_F}$ with T_F as the freeze-out temperature, g_* denotes the number of effective relativistic degrees of freedom at the time of freeze-out. DM particles with electroweak scale mass and couplings freeze out at temperatures in the range $x_F \approx 20 - 30$. This in turn simplifies to, as shown by the authors in [38],

$$\Omega_\chi h^2 \approx \frac{3 \times 10^{-27} cm^3 s^{-1}}{< \sigma v >}. \tag{2.6.3}$$

For complex scalar DM, the annihilation rate is given by Eq. (2.6.4). The relic abundance is related to the cross section of the DM-DM interaction. The terms in Eq. (2.3.1) evinces the interaction shown by figure 2.2. While finding the allowed parameter space satisfying the correct relic abundance and neutrino oscillation parameters we vary the Relic mass and the Majorana fermion mass(the right handed neutrino) both of which are involved in the cross section formula as shown in [39] reads as

$$(\sigma v)^{\chi\chi^\dagger}_{complex scalar} = \frac{v^2 y^4 m_\chi^2}{48\pi (m_\chi^2 + m_\psi^2)^2}. \tag{2.6.4}$$

With v = relative velocity of the two relic particles and is typically $0.3c$ at the freeze out temperature, χ is the relic particle (DM), y is the Yukawa coupling, m_χ the mass of the relic, m_ψ is the mass of the mediator particle. The dark

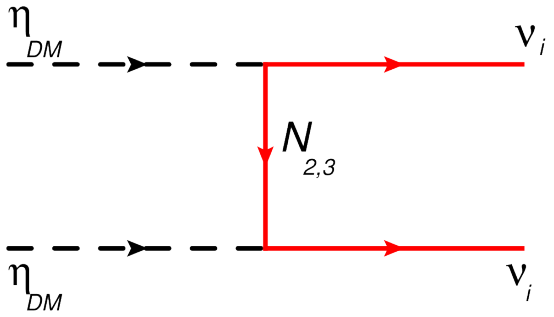

Figure 2.2: Feynman diagram showing the scattering of η_2 and η_3.

matter relic abundance may get affected by some kind of annihilation processes which might have taken place between the two neutral scalars depending on their mass difference $\Delta m = m_{\eta_2} - m_{\eta_3}$. If the mass splitting has the same order with the freeze-out temperature, the co-annihilation between the two neutral scalars play a significant role in finding the dark matter relic abundance. But if Δm is

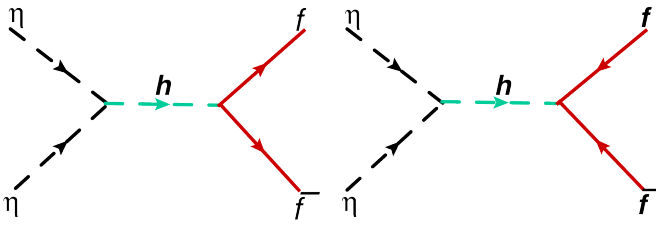

Figure 2.3: Self annihilation of η_2 and η_3 into SM fermions (conventions are followed from [41]).

larger than the freeze-out temperature, then the immediate heavier neutral scalar affects the dark matter relic density notably. The self annihilation between dark matter and immediately heavier component of the scalar triplet η contribute to the dark matter annihilation cross section. Many authors in [34, 36, 40] explored this kind of self annihilation consequences on dark matter relic abundance. To compute the effective annihilation cross section we are following the analysis done by the authors in [34]. The relevant annihilation channels and interactions can be given by figure 2.3. For low mass scheme ($m_{DM} < M_W$), the self annihilation of either η_2 or η_3 into SM particles takes place via the SM Higgs, which is depicted in figure 2.3. The according annihilation cross section [36, 40] is followed by Eq. (2.6.5).

$$\sigma_{xx} = \frac{|Y_f|^2|\lambda_x|^2}{16\pi s}\frac{(s-4m_f^2)^{3/2}}{\sqrt{s-4m_x^2}((s-m_h^2)^2+m_h^2\Gamma_h^2)}, \tag{2.6.5}$$

where $x \to \eta_{2,3}$, the coupling of x with SM Higgs h is denoted by λ_x and Y_f implies the fermion Yukawa coupling, which has been estimated to be 0.32 albeit the full possible range of values is $\lambda_f = 0.26 - 0.63$ [6]. $\Gamma_h = 4.15MeV$ is the decay width of the SM Higgs, m_h is 126 GeV. s is the thermally averaged center of mass squared energy given by

$$s = 4m^2 + m^2v^2. \tag{2.6.6}$$

where, v is the relative velocity and m is the mass of the relic. In order to yield the correct relic abundance we need to constrain the Yukawa coupling along with the relic mass and the mediator mass. Similar to the works done in [42, 43] here also we suppose the neutral component of the scalar triplet as the DM candidate. We choose the relic mass as lighter than the W boson mass $m_{DM} \leq M_W$. And

interestingly for the relic mass is kept in a comparatively smaller mass scale which is around 50 GeV. The mediator mass here in our case, i.e., the Majorana neutrino mass is required to vary from 153 GeV to 154 Gev to obtain the observed relic density. This type of findings have been extensively studied in the literature [39, 44]. For a light DM with a mass below 10 GeV, the LHC searches have a better awareness for complex scalar DM cases. Moreover, the LHC has a better reach than direct detection experiments with DM masses up to around 500 GeV for the complex scalar DM case.

2.7 Numerical analysis

The latest global fit [45] value with their best fit point (bfp) for 3σ range of neutrino oscillation parameters used to study neutrino phenomenology are given in Table 2.2 and Table 2.3: Cosmological constraint says that,

Oscillation parameters	bfp	3σ Cl
$\Delta m^2_{21}[10^{-5}eV^2]$	7.5	$(7.02, 8.07)$
$\Delta m^2_{31}[10^{-3}eV^2]$	2.457	$(2.317, 2.607)$
$\sin^2\theta_{12}$	0.304	$(0.270, 0.344)$
$\sin^2\theta_{13}$	0.0218	$(0.0186, 0.0250)$
$\sin^2\theta_{23}$	–	0.381-0.643

Table 2.2: Neutrino Oscillation data for Normal mass Ordering

Oscillation parameters	bfp	3σ Cl
$\Delta m^2_{21}[10^{-5}eV^2]$	7.5	$(7.02, 8.07)$
$\Delta m^2_{23}[10^{-3}eV^2]$	-2.449	$-2.590, -2.307$
$\sin^2\theta_{12}$	0.304	$0.270, 0.34$
$\sin^2\theta_{13}$	0.0219	$0.0188, 0.0251$
$\sin^2\theta_{23}$	–	$0.388, 0.644$

Table 2.3: Neutrino Oscillation data for Inverted mass Ordering

$$m_1 + m_2 + m_3 \leq 0.23eV.$$

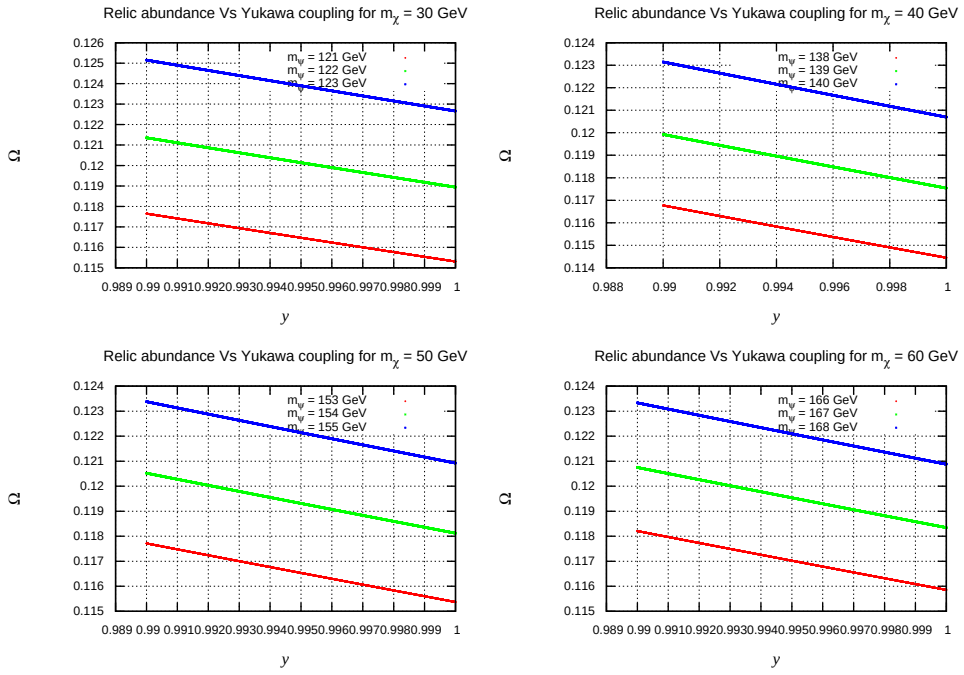

Figure 2.4: Variation of relic abundance with Yukawa coupling.

The Yukawa coupling governing the interaction is present in the established mathematical expression which computes the scattering cross section of this interaction in turn the relic abundance of the potential DM. As a proper choice of Yukawa coupling, the mediator mass along with the complex scalar mass allows us to achieve the observed relic abundance we need to put constraints on them. In our work we first fix the above mentioned parameters to get the relic abundance which is reported by PLANCK 2013 data. Fixing the relic mass around 50 GeV and varying the mediator mass from 153 to 154 GeV we get the idea of Yukawa coupling yielding the correct relic abundance. Since the required relic abundance for the potential DM candidate desires a mediator mass at a much lower scale (around 153 GeV), the ISS realization helps us in this regard (which is here, the mediator particle governing the t-channel scattering as shown in figure 2.2). The Yukawa coupling needs to fall between 0.99 to 1 to have a better reach of the relic abundance as shown in figure 2.4. We redefine the parameters of the matrix shown by the Eq. (2.3.5) in terms of p, q and r. Where, $p = \frac{ax_1\sqrt{\mu_1}}{M_1}$, $q = \frac{ax_2\sqrt{\mu_1}}{M_1}$ and $r = \frac{ax_3\sqrt{\mu_1}}{M_1}$. From the requirement of bringing the light neutrino mass matrix into TBM form we equate the 11-element of m_ν to $2q^2 - pq$ [9]. This

is done in accordance with adjusting the Yukawa couplings and the associated VEVs. Along with this redefenition we also make $q = r$ by $x_2 = x_3$ for numerical analysis. This structure of light neutrino mass matrix leads to a neutrino mass spectrum which is of inverted hierarchical type and a zero eigenvalue with $m_3 = 0$. For numerical analysis we take another couple of definitions for the Yukawa couplings $x_1 = x$ and $x_2 = x_3 = y$. We have kept $x = 1$ and varied y for computing the oscillation parameters and m_ν^{ee}, however there is no significant changes observed by keeping y fixed and varying x. Each value of y gives rise to various sets of the neutrino mass matrix parameters p, q. We parameterize the light neutrino mass matrix obtained from the ISS realization with the help of recent neutrino oscillation data given in Table 2.2 and Table 2.3. Along with the redefined parameters of the light neutrino mass matrix and using Eq. (2.3.2), Eq. (2.3.3) and Eq. (2.3.4) the new light neutrino mass matrix is found to be of TBM type given by Eq. (2.7.1)

$$m_\nu = \begin{pmatrix} 2q^2 - pq & pq & pq \\ pq & q^2 & q^2 \\ pq & q^2 & q^2 \end{pmatrix}. \tag{2.7.1}$$

We have analyzed the model only for IH case as the light neutrino mass matrix structure only allows us to have the inverted hierarchy mass pattern. After diagonalizing the complete mass matrix the mass eigenvalues are found to be $m_1 = -2(pq - q^2)$, $m_2 = q(p + 2q)$ and $m_3 = 0$. Then we parametrize the mass matrix keeping $x = 1$ while at the same time varying y between a range around $0.994 - 1$. Choosing each set of p, q values which have been found different for different "y" values, we get several light neutrino mass matrices. The same Yukawa coupling y is being varied in the dark matter sector too for showing its contribution to obtain the correct relic abundance. For the generation of non-zero reactor mixing angle, we include type II correction [25] to the leading order neutrino mass matrix as explained in Section 2.4. This perturbation brings out non-zero θ_{13} in 3σ range along with $m_3 \neq 0$ leaving the light neutrino masses with IH nature only. The numerical value of the perturbation term $w = f_\nu v_\Delta$ critically depends upon the Majorana coupling f_ν, trilinear mass parameter $\mu\phi\Delta$,

and M. Accordingly, we vary the type II seesaw strength from 10^{-6} to 0.01 to produce non-zero θ_{13}. It is observed from the figure 2.5 that, the type II seesaw strength of 10^{-3} eV is generating the non-zero θ_{13} in the 3σ range in all cases. The perturbation matrix takes the following structure.

$$m_\nu^{II} = \begin{pmatrix} 0 & -w & w \\ -w & w & 0 \\ w & 0 & -w \end{pmatrix},$$

After adding the perturbation we get the neutrino mass matrix as follows.

$$m_\nu = m_\nu^I + m_\nu^{II}.$$

Now the elements of these diagonalized matrices are associated with the parameters of the model and the type II perturbation term. The set of p, q values obtained for each y value and chosen for analysis are listed in Table 2.4, Table 2.5 and Table 2.6. In addition p, q corresponds to some complex sets of solution too. Taking them under consideration, no significant changes in the numerical analysis have been noticed.

A comparison among the various sets of results obtained in the DM phenomenology part has been made in Table 2.7 and neutrino phenomenology has been shown in the Table 2.8. The light neutrino mass matrix (2.7.1) is having only

Parameters	$y = 0.994$	$y = 0.996$	$y = 0.998$	$y = 1$
p	0.366138	0.366146	0.366154	0.357719
q	0.0899502	0.089768	0.0895865	0.091516

Table 2.4: Values of p, q obtained by solving for IH case with best fit central value of 3σ deviations

two unknown parameters, solution for which demands two equations. Two mass squared differences which we get from neutrino oscillation data, lead to those two parameters. Then using the solutions for p and q the light neutrino mass matrix is obtained. Then we fix the mass eigenvalues from that light neutrino mass matrix.

Parameters	$y = 0.994$	$y = 0.996$	$y = 0.998$	$y = 1$
p	0.371351	0.371359	0.371367	0.362663
q	0.0911924	0.0910077	0.0908236	0.0928181

Table 2.5: Values of p, q obtained by solving for IH case with a upper bound of 3σ deviations

Parameters	$y = 0.994$	$y = 0.996$	$y = 0.998$	$y = 1$
p	0.360693	0.3607	0.360708	0.352452
q	0.088626	0.0884465	0.0882677	0.0901551

Table 2.6: Values of p, q obtained by solving for IH case with an lower bound of 3σ deviations

Using the best fit central values from the oscillation data, we numerically fit the leading order neutrino mass matrix. A thorough analysis has been carried out to check whether the oscillation parameters are near to reach or not by taking the upper and lower bound of 3σ deviation as well. Here we try to exhibit an unexplored parameter space satisfying both the DM relic abundance and neutrino phenomenology.

The scattering cross section of the decay channel described by figure 2.3 to various SM fermions have been calculated. They are found to have an order of 10^{-60}cm^2 / 10^{-42}GeV^{-2} which is much smaller than the cross section which has been achieved for the t-channel contribution (of the order of 10^{-44}cm^2). They will have little contribution (can be neglected therefore) to the relic abundance of the potential DM candidate. We have already noticed that for obtaining the observed Ω we need to fix the Yukawa coupling. Fixing the Yukawa coupling as varying from 0.99 to 1, varying m_{DM} from 30 to 60 GeV and varying M_R from 120 to 167 GeV, we study the order of relic abundance. We fit the values of oscillation parameters using recent cosmological constraints for inverted mass ordering. We compute all the oscillation parameters also by varying the type II seesaw strength. Variation of type II seesaw strength with the non-vanishing θ_{13}, has been shown in figure 2.5 and figure 2.6. The production of other oscillation parameters, e.g. the two mixing angles and two mass squared splitting as a function of nonzero θ_{13} has been

shown in the figure 2.7, figure 2.8 and figure 2.9 for different values of Yukawa coupling. The sum of absolute masses has also been calculated to see whether it satisfies the Planck upper bound or not. Seeing that, the sum of absolute neutrino masses can give some clue on neutrinoless double beta decay, a little study has been performed to check whether the presented model is able to contribute to the $0\nu\beta\beta$ physics. In figure 2.10 we plot for the contribution of the effective mass to $0\nu\beta\beta$ decay due to light neutrino exchanges for standard contribution showing the variation of effective mass with the type II seesaw strength. Figure 2.11 displays the variation of m_ν^{ee} with the lightest neutrino mass, in our model m_3. In figure 2.12 we present the variation of effective mass with $m_{lightest}$ and type II seesaw strength taking the upper and lower bound of 3σ deviation. Since the presented model only present a hierarchy of inverted kind the lowest mass range has been selected which is resulted from the perturbation. The variation in m_ν^{ee} for non-standard contribution with different y values have been checked and found to be in agreement with the experimental bounds. The effective mass for non-standard contribution has been obtained around 0.0489 almost for all the values of Yukawa couplings chosen for the analysis. It is worth noting that the variation in Yukawa coupling leaves trivial impacts on m_ν^{ee} for non-standard contribution. For showing the variation of m_ν^{ee} with m_3, we choose those values of m_3 obtained as a result of adding the type II seesaw strength.

The following observations have been made from the results and analysis.

- The relic abundance has been found to match the value shown by PLANCK 2013 data, for a choice of Yukawa coupling ranging from 0.99 to 1 provided the Relic mass is fixed at 50 GeV keeping the mediator mass at a range from 153 to 154 GeV. A detailed analysis of the choice of Yukawa coupling, the Relic mass (m_χ) and the mediator mass (m_ψ) for this particular model has been presented in the Table 2.7.

- The oscillation parameters are near to reach only when the Yukawa coupling is varied from 0.994 to 1 and as a further increase/decrease of the Yukawa coupling does not yield good neutrino phenomenology we have considered

m_χ	m_ψ	y	Ω
30 GeV	$(121-122)$ GeV	$(0.99-1)$	✓
40 GeV	139 GeV	$(0.99-1)$	✓
50 GeV	$(153-154)$ GeV	$(0.99-1)$	✓
60 GeV	$(166-167)$ GeV	$(0.99-1)$	✓

Table 2.7: Comparison of relic abundance Ω with various choices of Yukawa couplings, DM mass, RH neutrino mass

3σ ranges	θ_{13}	θ_{12}	θ_{23}	Δm^2_{21}	Δm^2_{23}	Σ mod m_i
bfp	✓	✓	✓	✓	✓	✓
lower bound	✓	✓	✓	✓	✓	✓
upper bound	✓	✓	✓	✓	×	✓

Table 2.8: Summary of results obtained from various allowed mass schemes.

those corresponding values of relic abundance obtained for Yukawa coupling ranging from 0.994 to 1.

- It has been noticed that the proposed model evidences correct neutrino phenomenology using the best fit and lower 3σ bound in case of inverted hierarchy mass pattern only. All the oscillation parameters have seen to come inside the frame while taking the the best fit and lower 3σ bound.

- The non-zero value of θ_{13} has been found to be consistent with the variation of type II seesaw strength.

- Both the standard and new physics contribution to $0\nu\beta\beta$ decay in the allowed hierarchy is obtained in the vicinity of experimental results [46].

2.8 Conclusion

An A_4 based IH neutrino mass model originating from both inverse and type II seesaw have been studied. Here ISS is implemented as a leading order contribution to the light neutrino mass matrix yielding zero reactor mixing and

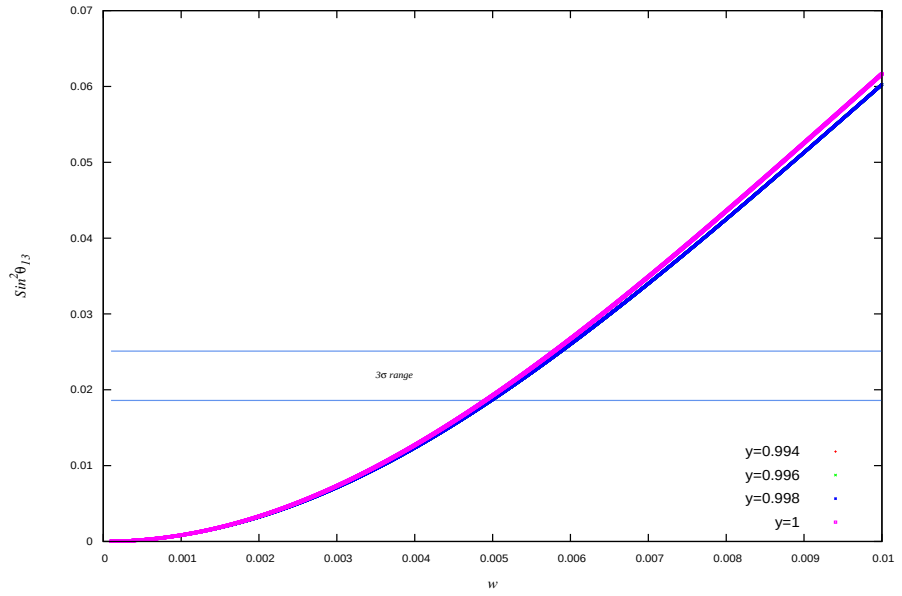

Figure 2.5: Generation of non-zero $sin^2\theta_{13}$ varying the type II strength for best fit values.

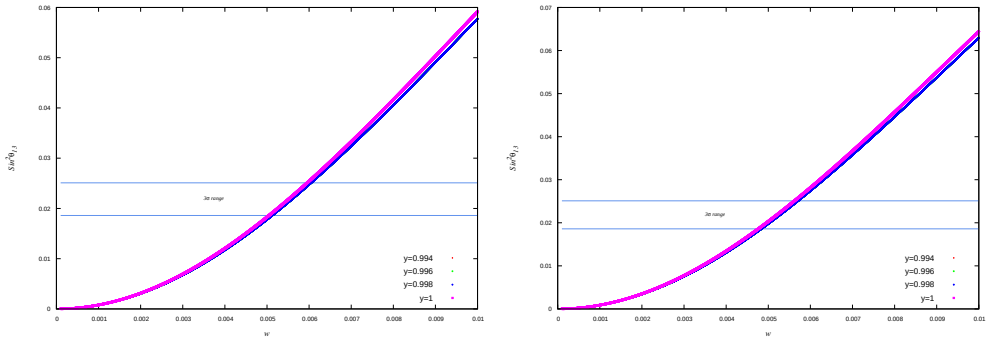

Figure 2.6: Generation of non-zero $sin^2\theta_{13}$, varying the type II strength using upper bound (left panel) and lower bound (right panel) of 3σ deviations.

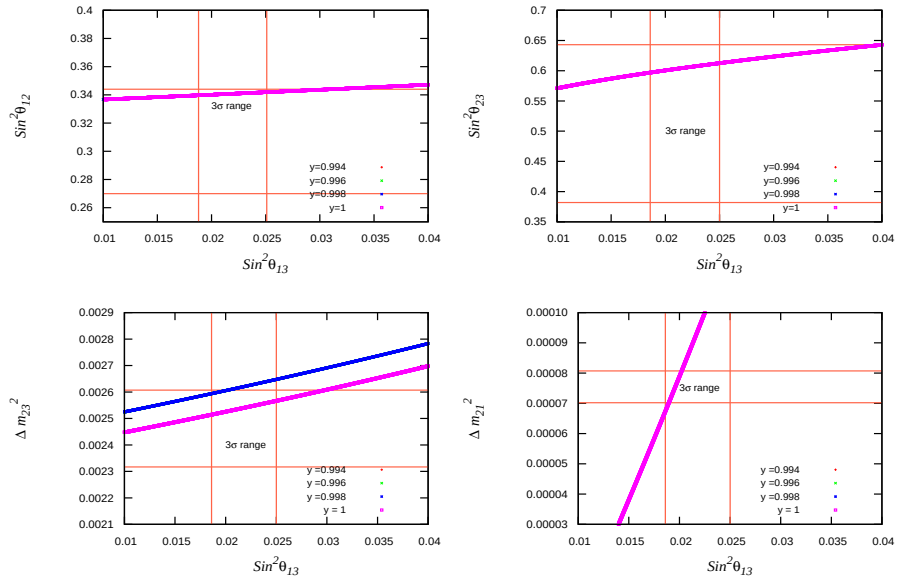

Figure 2.7: Variation of $sin^2\theta_{12}$, $sin^2\theta_{23}$,Δm^2_{23} and Δm^2_{21} with $sin^2\theta_{13}$ with best fit value.

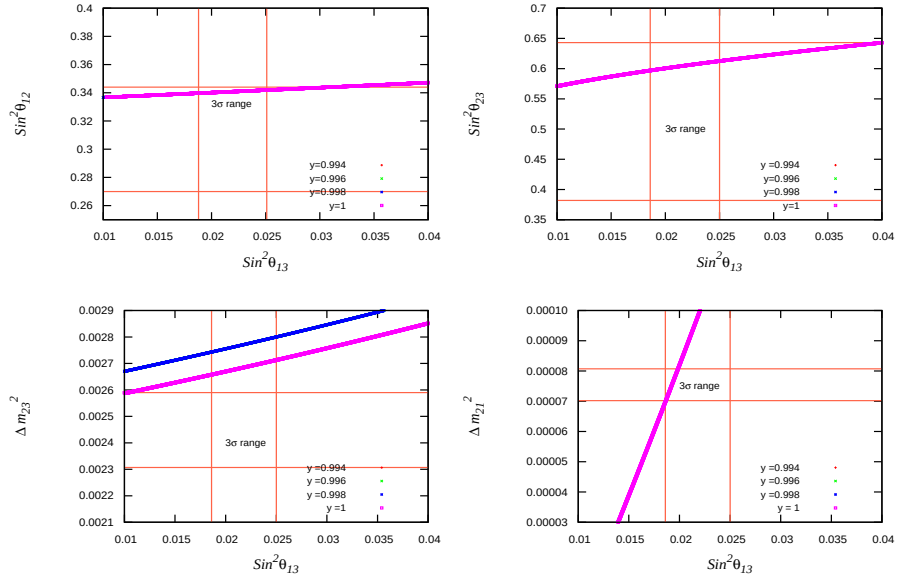

Figure 2.8: Variation of $sin^2\theta_{12}$, $sin^2\theta_{23}$,Δm^2_{23} and Δm^2_{21} with $sin^2\theta_{13}$ with upper bound of 3σ deviation.

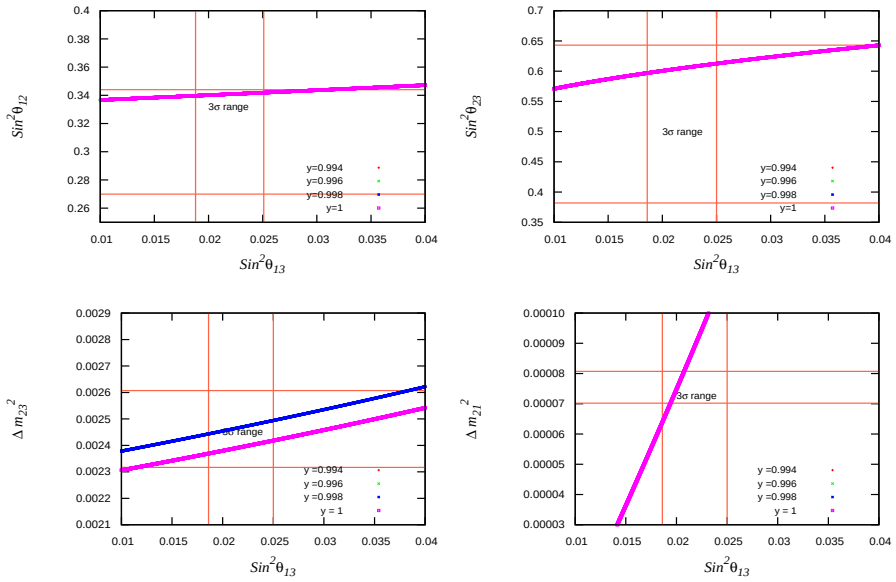

Figure 2.9: Variation of $sin^2\theta_{12}$, $sin^2\theta_{23}$,Δm^2_{23} and Δm^2_{21} with $sin^2\theta_{13}$ with lower bound of 3σ deviation.

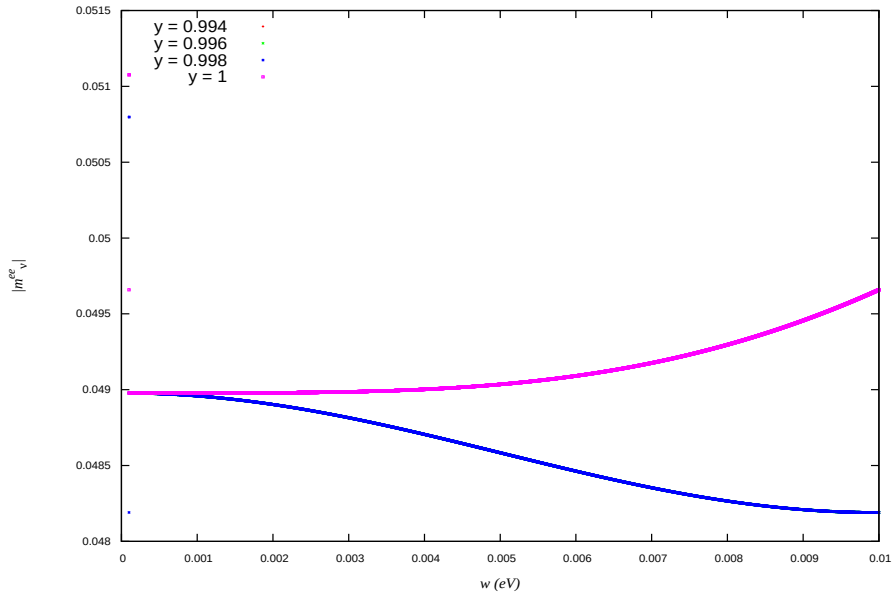

Figure 2.10: Variation of effective mass m_ν^{ee} (in eV) with type II seesaw strength using bfp.

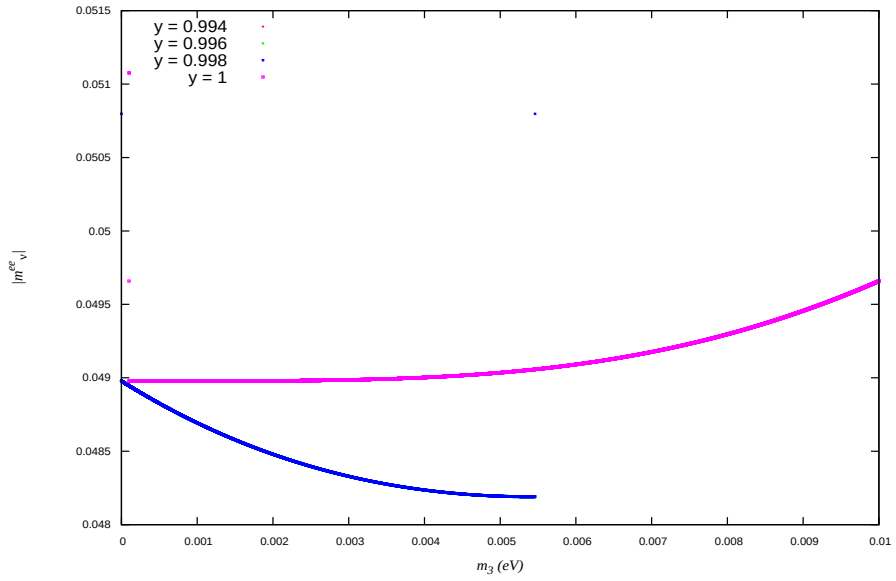

Figure 2.11: Variation of effective mass m_ν^{ee} (in eV) with the lightest neutrino mass using bfp.

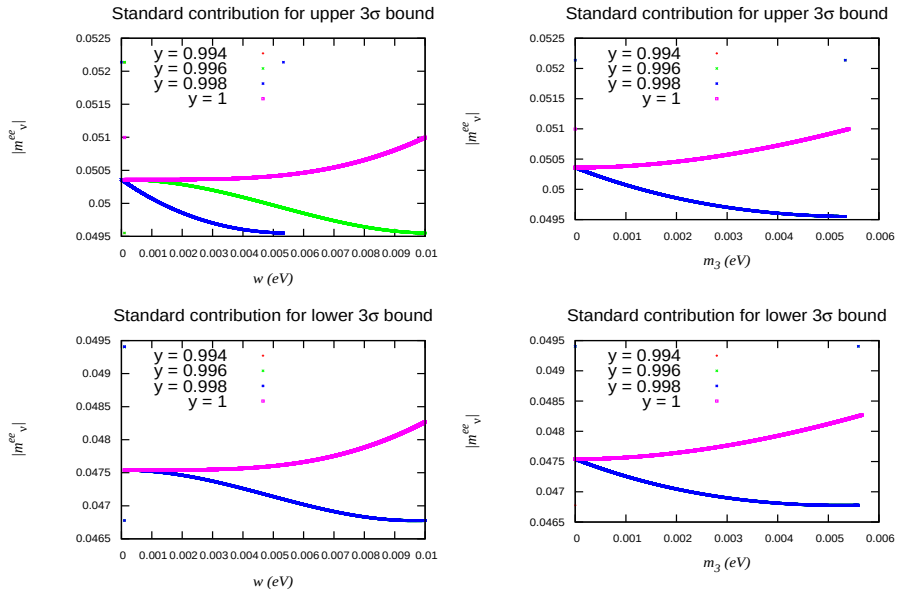

Figure 2.12: Variation of effective mass m_ν^{ee} (in eV) with type II seesaw strength and the m_3 for upper and lower 3σ bounds.

$m_3 = 0$. Then the type II seesaw has been used in order to produce non-Zero reactor mixing angle, which later on produces $m_3 \neq 0$ keeping the hierarchy as inverted only. We have studied the possibility of having a common parameter space where both the Neutrino oscillation parameters in the 3σ range and DM

relic abundance has a better reach. With a proper choice of Yukawa coupling(y), right handed neutrino (mediator particle) mass (m_ψ) , and complex scalar (potential DM candidate) mass (m_χ) the variation in relic abundance as a function of Yukawa coupling has been shown. For a choice of Yukawa coupling between 0.994 to 0.9964, m_{DM} around 50 GeV, the mediator mass needs to fall around 153 GeV to match the correct relic abundance. The same Yukawa coupling has got a key role in generating the Neutrino oscillation parameters as well. We have studied the prospect of producing non-zero θ_{13} by introducing a perturbation to the light neutrino mass matrix using type II seesaw within the A_4 model. We have also determined the strength of the type II seesaw term which is responsible for the generation of non-zero θ_{13} in the correct 3σ range. We have also checked whether the proposed model can project about neutrinoless double beta decay or not. In context to the presented model we have found a wide range of parameter space where one may have a better reach for both neutrino and dark matter sector as well. This model may have relevance in studying baryon asymmetry of the universe, which we leave for future study.

Bibliography

[1] Berlin, A., Gori, S., Lin, T., and Wang, L. Pseudoscalar portal dark matter, *Physical Review D*, 92:015005, 2015.

[2] Begeman, K. G., Broeils, A. H., and Sanders, R. H. Extended rotation curves of spiral galaxies : dark haloes and modified dynamics, *Monthly Notices of the Royal Astronomical Society*, 249: 523B, 1991.

[3] Bradac, M.,Clowe, D., Gonzalez, A. H., Marshall, P., Forman, W., Jones, C., Markevitch, M., Randall, S., Schrabback, T., and Zaritsky, D. Strong and weak lensing united. III. Measuring the mass distribution of the merging galaxy cluster 1ES 0657-558. *Astrophysical Journal*, 652(2):937-947, 2006.

[4] Bennett, C. L., et al. Nine-year Wilkinson Microwave Anisotropy Probe (WMAP) observations : final maps and results. *The Astrophysical Journal Supplement Series*, 208(2):20, 2013.

[5] Ade, P. A. R., et al. Planck 2013 results. XVI. Cosmological parameters. *Astronomy and Astrophysics*, 571:A16, 2014.

[6] Dasgupta, A. and Borah, D. Scalar dark matter with type II seesaw. *Nuclear Physics B*, 889:637-649, 2014.

[7] Taoso, M., Bertone, G., and Masiero, A. Dark Matter Candidates: A Ten-Point Test. *Journal of Cosmology and Astroparticle Physics*, 03:022, 2008.

[8] Fraser, S., Ma, E., and Zakeri, M. $SU(2)_N$ Model of Vector Dark Matter with a Leptonic Connection. *International Journal of Modern Physics A*, 30(03):1550018, 2015.

[9] Hirsch, M., Morisi, S., Peinado, E., and Valle, J. W. F. Discrete dark matter. *Physical Review D*, 82(11):116003(1)–116003(5), 2010.

[10] Meloni, D., Morisi, S., and Peinado, E. Neutrino phenomenology and stable dark matter with A_4. *Physics Letters B*697(4):339-342, 2011.

[11] Ma, E. Dark Scalar Doublets and Neutrino Tribimaximal Mixing from A_4 Symmetry. *Physics Letters B*, 671(3):366-368, 2009.

[12] Dias, A. G., de S. Pires, C. A., and da Silva, P. S. R. How the inverse seesaw mechanism can reveal itself natural, canonical, and independent of the right-handed neutrino mass. *Physical Review D*, 84(5):053011, 2011.

[13] Mohapatra, R. N. and Valle, J. W. F. Neutrino mass and baryon-number nonconservation in superstring models. *Physical Review D*, 34(5):1642-1645, 1986.

[14] Mohapatra, R. N. Mechanism for Understanding Small Neutrino Mass in Superstring Theories. *Physical Review Letters*10(6):56, 1986.

[15] Dias, A. G., de S. Pires, C. A., da Silva, P. S. R., and Sampieri, A. A Simple Realization of the Inverse Seesaw Mechanism. *Physical Review D*, 86(3):035007, 2012.

[16] Malinsky, M., Ohlsson, T., and Zhang, H. Nonunitarity effects in a realistic low-scale seesaw model. *Physical Review D*, 79(7):073009, 2009.

[17] Ma, E. Radiative inverse seesaw mechanism for nonzero neutrino mass. *Physical Review D*, 80(1): 013013, 2009.

[18] Dev P. S. B. and Mohapatra R. N. TeV scale inverse seesaw model in SO(10) and leptonic nonunitarity effects. *Physical Review D*, 81(1):013001, 2010.

[19] Dev P. S. B. and Pilaftsis, A. Minimal radiative neutrino mass mechanism for inverse seesaw models. *Physical Review D*, 86(11):113001, 2012.

[20] Altarelli, G. and Feruglio, F. Tri-bimaximal neutrino mixing, A_4 and the modular symmetry. *Nuclear Physics B*, 741(1-2):215-235, 2006.

[21] Altarelli, G. and Feruglio, F. Discrete flavor symmetries and models of neutrino mixing. *Reviews of Modern Physics*, 82:2701, 2010.

[22] Ma, E. Tribimaximal neutrino mixing from a supersymmetic model with A_4 family symmetry. *Physical Review D*, 73(5):057304, 2004.

[23] Brahmachari, B., Choubey, S., and Mitra, M. A_4 flavor symmetry and neutrino phenomenology. *Physical Review D*, 77(7):073008, 2008.

[24] Varzielas, I. de M. and Fischer, O. Non-Abelian family symmetries as portals to dark matter. *Journal of High Energy Physics*, 01:160, 2016.

[25] Borah, M., Borah, D., Das, M. K., and Patra, S. Perturbations to the $\mu-\tau$ symmetry, leptogenesis and lepton flavor violation with the type II seesaw mechanism. *Physical Review D*, 90(9):095020, 2014.

[26] Ma, E. and Sarkar, U. Neutrino Masses and Leptogenesis with Heavy Higgs Triplets. *Physical Review Letters*, 80(26):5716, 1998.

[27] Rodejohann, W. Type II See-Saw Mechanism, Deviations from Bimaximal Neutrino Mixing and Leptogenesis. *Physical Review D*, 70(7):073010, 2004.

[28] Lindner, M. and Rodejohann, W. Large and Almost Maximal Neutrino Mixing within the Type II See-Saw Mechanism. *Journal of High Energy Physics*, 05:089, 2007.

[29] Borah, D. Deviations from tri-bimaximal neutrino mixing using type II seesaw, *Nuclear Physics B*, 876(2):575-586, 2013.

[30] Borah, D. Patra, S., and Pritimita, P. Sub-dominant type-II seesaw as an origin of non-zero θ_{13} in $SO(10)$ model with TeV scale Z gauge boson, *Nuclear Physics B*, 881: 444-466, 2014.

[31] Rodejohann, W., Neutrino-less double beta decay and particle physics *International Journal of Modern Physics E* , 20(09):1833, 2011.

[32] Klapdor-Kleingrothaus, H. V., Dietz, A., Harney, H. L., and Krivosheina, I. V. Evidence for neutrinoless double beta decay. *Modern Physics Letters A*, 16:2409, 2001.

[33] Bilenky,S. M. and Giunti, C. Neutrinoless double beta decay: A brief review. *Modern Physics Letters A*, 27(13):1230015, 2012.

[34] Griest, K. and Seckel, D. Three exceptions in the calculation of relic abundances. *Physical Review D*, 43(10):191-3203, 1991.

[35] Kolb, E. W. and Turner, M. S. *The Early Universe*. Elsevier Inc., San Diego, CA. pages 1-547, 1990.

[36] Edsjo, J. and Gondolo, P. Neutralino relic density including coannihilations. *Physical Review D*, 56(4):1879-1894, 1997.

[37] Gelmini, G. and Gondolo, P. Cosmic abundances of stable particle: Improved analysis. *Nuclear Physics B*, 360:145-179, 1991.

[38] Jungman, G., Kamionkowski, M., and Griest, K. Supersymmetric dark matter. *Physics Reports*, 267(5-6):195-373, 1996.

[39] Bai, Y. and Berger, J. Fermion Portal Dark Matter. *Journal of High Energy Physics*, 11:171, 2013.

[40] Bell, N. F., Cai, Y., and Medina, A. D. Co-annihilating Dark Matter: Effective Operator Analysis and Collider Phenomenology. *Physical Review D*, 89(11):115001, 2014.

[41] Dreiner, H. K., Haber, H. E., and Martin, S. P. Two-component spinor techniques and Feynman rules for quantum field theory and supersymmetry. *Physics Reports*, 494:1, 2010.

[42] Boucenna, M. S., Morisi, S., Peinado, E., Valle, J. W. F., and Shimizu, Y. Predictive discrete dark matter model and neutrino oscillations. *Physical Review D*, 86(7), 073008, 2012.

[43] Boucenna, M. S., Hirsch, M., Morisi, S., Peinado, E., Taoso, M., and Valle, J. W. F. Phenomenology of Dark Matter from A_4 Flavor Symmetry. *Journal of High Energy Physics*, 05:037, 2011.

[44] Bai, Y. and Berger, J. Lepton Portal Dark Matter. *Journal of High Energy Physics*, 08:153, 2014.

[45] Bergstrom, J., Gonzalez-Garcia, M. C., Maltoni, M., and Schwetz, T. Bayesian Global analysis of neutrino oscillation data, *Journal of High Energy Physics*, 1509:200, 2015.

[46] Agostini, M., et al. Search of Neutrinoless Double Beta Decay with the GERDA Experiment. In *37th International Conference on High Energy Physics (ICHEP 2014)*, volumes(273-275), pages 1876-1882, Valencia, Spain, 2-9 Jul 2014. Elsevier.